Control of North Atlantic deep water circulation by the Greenland-Scotland ridge

ARTICLE *in* PALEOCEANOGRAPHY · APRIL 1996

Impact Factor: 3.92 · DOI: 10.1029/95PA03696

2 AUTHORS:

James D Wright
Rutgers, The State University of New Jersey

Kenneth G. Miller
Rutgers, The State University of New Jersey

PALEOCEANOGRAPHY, VOL. 11, NO. 2, PAGES 157-170, APRIL 1996

Control of North Atlantic Deep Water circulation by the Greenland-Scotland Ridge

James D. Wright[1]
Lamont-Doherty Earth Observatory, Palisades, New York

Kenneth G. Miller
Department of Geological Sciences, Rutgers University, Piscataway, New Jersey
Lamont-Doherty Earth Observatory, Palisades, New York

Abstract. Coherent bathymetric features along the Reykjanes Ridge indicate that there were significant changes in the flux of buoyant material within the Icelandic Hot Spot during the Neogene. The radial extent of the topographic swell associated with this hot spot is of the order of 1000 to 2000 km, and therefore these changes affected the Greenland-Scotland Ridge (GSR). At present, sill depths along the GSR are generally less than 500 m with the deepest passage being less than 1000 m, making the overflow water sensitive to even small changes in the ridge depths. Reconstructions of Neogene mantle plume activity correlate with the deepwater circulation patterns in the North Atlantic. Times of high mantle plume activity caused Northern Component Water (NCW) production to cease. NCW fluxes resumed once this phase of high mantle plume activity slowed. The long-term climate change during the Neogene must be controlled by factors other than NCW production. However, climatic optima during the late early Miocene and early Pliocene appear to have been augmented by high NCW fluxes, while subsequent middle Miocene and "middle" Pliocene coolings correlate with uplifts on the GSR and reduced NCW flux. We suggest that reductions in NCW may have contributed to both of these cooling events.

Introduction

Global climate changes during the Cenozoic may be related to plate tectonic changes that disrupted the stability of the climate system, including rearranging continental positions, building mountain ranges, and opening/closing whole ocean basins. *Berger et al.* [1981] noted that the link between tectonics and climate is elusive because the timing of tectonic changes is poorly constrained versus the relatively precise dating of climatic changes. Nevertheless, paleoceanographers have and will continue to seek tectonic explanations for climatic events, especially for the longer-term (m.y. to 10 m.y. scale) changes. Recent studies have linked Miocene and Pliocene glaciations to tectonic uplift of the Tibetan Plateau [*Ruddiman et al.*, 1989; *Raymo and Ruddiman*, 1992]. Deep-sea records provide a detailed chronology of each of these climatic events: (1) while ice sheets grew and decayed in the Oligocene to early Miocene, the permanent Antarctic Ice Sheet was established in the middle Miocene between 15 and 12.5 Ma [*Shackleton and Kennett*, 1975; *Savin et al.*, 1975; *Miller et al.*, 1991]; and (2) while Northern Hemisphere Glaciation (NHG) began prior to the Pliocene, it increased around 3.2 Ma and evolved into large-scale glacial cycles by 2.6 Ma [*Shackleton and Opdyke*, 1977; *Raymo et al.*, 1989; *Bohrmann et al.*, 1991; *Larsen et al.*, 1994]. Validation of orographic effects still requires better constraints on the timing and magnitude of uplift in these regions [*Ruddiman et al.*, 1989; *Molnar and England*, 1990] and further evaluation of possible climatic consequences [c.f. *Raymo et al.*, 1988; *Berner et al.*, 1983].

Early work on climate change and tectonics focused on the role of the Greenland-Scotland Ridge (GSR) [e.g., *Vogt*, 1972; *Schnitker*, 1980] and its potential effects on climate through a link with North Atlantic Deep Water (NADW). Sill depths along the GSR are important because this ridge separates the North Atlantic from the colder, more dense waters in the Arctic Ocean and Norwegian-Greenland Seas, and therefore it is a critical gateway affecting Cenozoic deepwater circulation patterns and climate change. Greenland-Scotland Ridge depths are generally less than 500 m with the deepest passage being 800 to 1000 m, making the overflow water sensitive to small variations in the ridge depth (Figure 1). *Vogt* [1972] predicted that the GSR reached a critical level during the early Miocene, allowing Northern Component Water (NCW, proto-NADW) to first flow over the sill into the northern North Atlantic at that time. Widespread lower Miocene drift deposits in the northern North Atlantic are consistent with this interpretation [*Jones et al.*, 1970; *Ruddiman*, 1972; *Shor and Poore*, 1979]. *Schnitker* [1980] proposed that the critical depths were not reached until the middle Miocene, suggesting that GSR subsidence allowed relatively warm NCW to upwell around Antarctica. The upwelled and relatively warm NCW provided a moisture source to build a large ice sheet on Antarctica as reflected by the major middle Miocene $\delta^{18}O$ increase.

[1]Now at Department of Geological Sciences and Institute for Quaternary Studies, University of Maine, Orono.

Paper number 95PA03696.
0883-8305/96/95PA-03696$10.00

a.

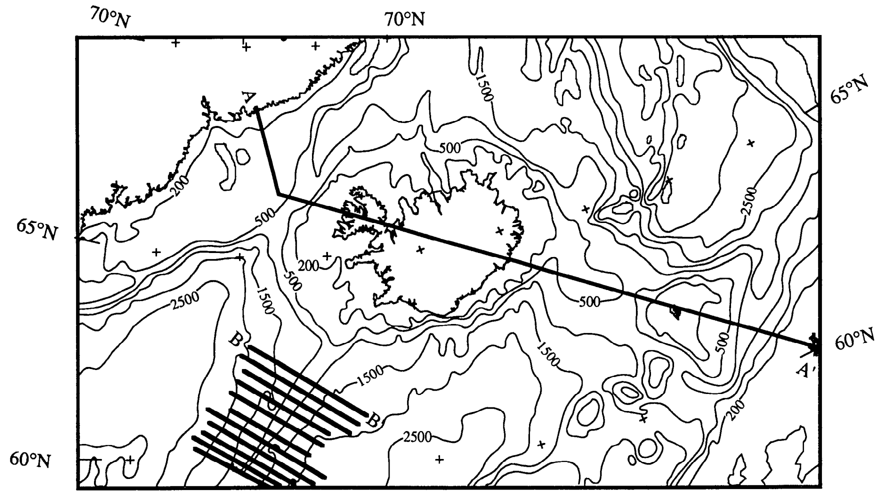

b.

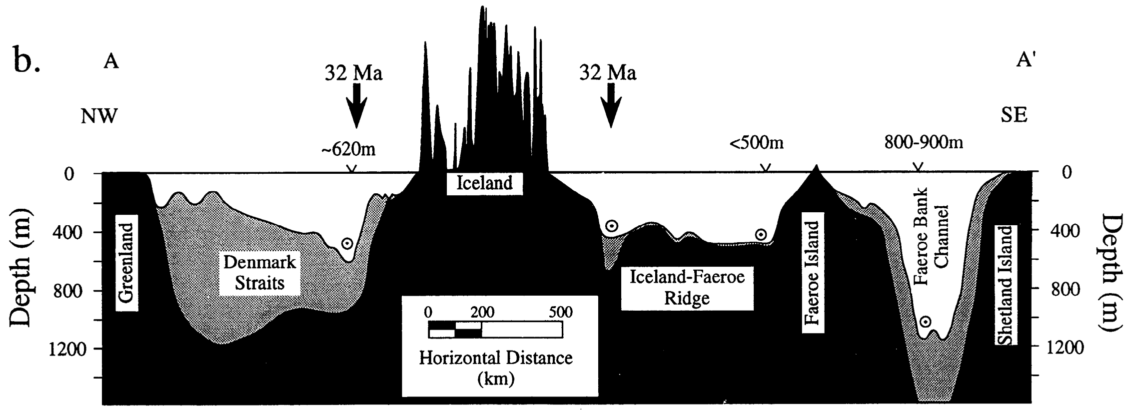

Figure 1. (a) Bathymetric map showing the regional features associated with the Icelandic mantle plume. The bathymetric contours begin with 200 and 500 m and continue at 500 m intervals. (b) The A-A' cross section shows the Greenland-Scotland Ridge (GSR) (modified from *Miller and Tucholke* [1983]). Sediment coverage is shaded in gray. The main conduits of water across the GSR are through the Denmark Strait (~600 m), on the Greenland-Iceland segment of the GSR, the Iceland-Faeroe overflow where water depths are ~500 m, and the Faeroe Bank Channel between the Faeroe Islands and Scotland. The GSR overflow to the east and west of Iceland is roughly equal.

In this paper, Greenland-Scotland Ridge subsidence over the past 25 m.y. is reconsidered. Simple thermal subsidence models [*Vogt*, 1972; *Talwani and Eldholm*, 1977; *Thiede and Eldholm*, 1983] are inappropriate for the GSR because the thermal history in this region appears to be more complicated. Evidence for this includes (1) the basement under the Greenland-Iceland portion of the ridge (Denmark Strait) is significantly deeper than the Iceland-Faeroe Ridge, and thermal subsidence models for the Greenland-Iceland Ridge must account for sediment loading [*Larsen*, 1983]; (2) the Faeroe-Shetland portion of the ridge is the deepest sill at present, and it is underlain by continental crust [*Ridd*, 1983]; and (3) there is evidence for episodes of increased mantle plume activity in the region, affecting the thermal subsidence [*Vogt*, 1971, 1983; *Vogt and Tucholke*, 1989]. Correlation of regional magnetic polarity patterns [*Nunns*, 1983] to the geomagnetic polarity timescale (GPTS) [*Cande and Kent*, 1992] and radiometric dating of lava sequences on Iceland provide a chronology for these episodes. As a result, tectonic events can be directly correlated with the deepwater circulation patterns in the North Atlantic [*Miller and Tucholke*, 1983; *Raymo et al.*, 1992; *Wright et al.*, 1992]. Finally, we evaluate causal links between GSR tectonics, deepwater circulation in the North Atlantic, and climate change over the past 25 m.y.

Regional Tectonics

The GSR is part of a mantle plume system centered under the Icelandic Plateau (Figure 1). High heat flow and low mantle densities under Iceland result in its subaerial exposure and the relatively shallow depths of other features proximal to Iceland [*Vogt*, 1971, 1974, 1983; *Vogt and Avery*, 1974; *Nunns*, 1983]. This regional swell associated with this mantle plume results from the injection of heat and buoyant mantle material into the less viscous asthenosphere that spreads out in a radial pattern below the crust [*White and McKenzie*, 1989; *Sleep*, 1990]. At present, the flux of buoyant material from the Iceland plume is moderately high and consequently, the radial extent of the swell or topographic anomaly is of the order of a thousand kilometers [*Anderson et al.*, 1973; *White and McKenzie*, 1989; *Sleep*, 1990; *Vogt et al.*, 1981; *Schilling*, 1986]. Past changes in the flux of heat and buoyant material from the mantle plume affected regional elevations surrounding Iceland, including the GSR.

Evidence from Iceland and the Reykjanes Ridge indicates that the mantle plume activity under Iceland has not been constant during the Neogene. Several coherent bathymetric features along the Reykjanes Ridge have a steplike appearance (Figure 2) [*Talwani et al.*, 1971; *Luyendyk et al.*, 1979]. These features have been attributed to fluctuations in plume activity under Iceland that propagated along the ridge axis [*Vogt*, 1971, 1974, 1983]. The most prominent of these features are paired vertical offsets or escarpments that have greater than 500 m relief on each side (Escarpments E and A, Figure 2). As part of the mid-ocean spreading system, the Reykjanes Ridge should follow a relatively predictable thermal subsidence [*Sclater et al.*, 1971]. The magnitude of these topographic

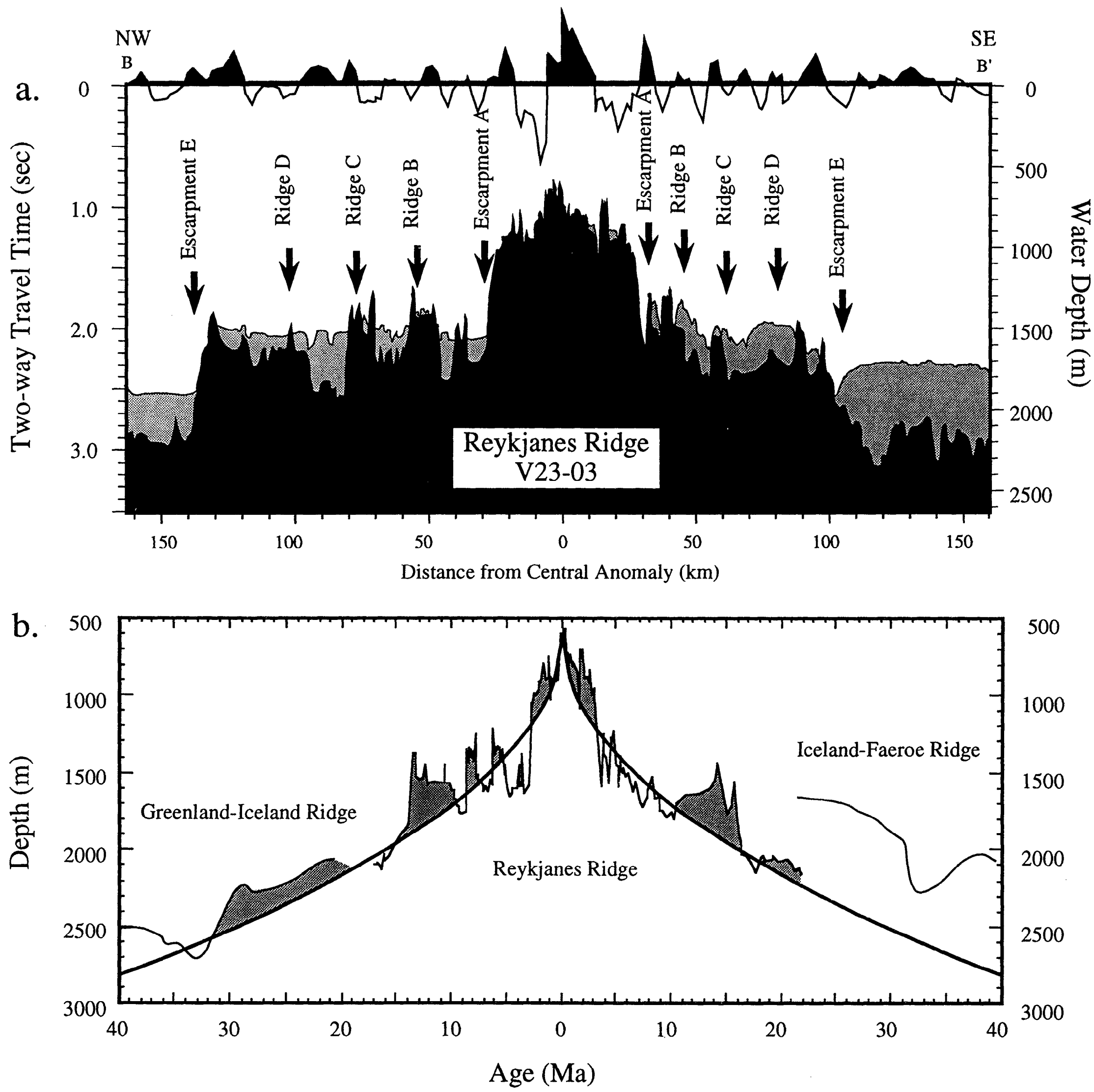

Figure 2. (a) Interpretation of V23-03 seismic transect across the Reykjanes Ridge. The location of this transect is shown in Figure 1a (B - B'). *Vogt* [1971] identified several coherent bathymetric features along the Reykjanes Ridge (Escarpments E and A; Ridges D, C, and B) and attributed these to changes in the Icelandic mantle plume discharge. The polarity patterns across the Reykjanes Ridge are shown above the cross section. (b) Crustal depths versus age for the Reykjanes and GSR were adjusted to account for the effects of sediment loading. The smooth curve radiating from 0 Ma is the predicted thermal subsidence curve which used a decay of $350 \times \sqrt{t}$. The initial starting depth used for this section across the Reykjanes Ridge was 600 m. The initial depth used for the GSR and Iceland-Faeroe Ridge was 1100 m above sea level. The difference between the GSR/Iceland Faeroe Ridge and Reykjanes Ridge initial depths is 1700 m and this value was subtracted from the GSR and Iceland Faeroe cross sections to compare to the Reykjanes Ridge cross section. Times when the crust was higher than the predicted depth are shaded in gray.

anomalies is more apparent when the corrected crustal depths are compared to the predicted thermal decay curves (Figure 2b) [*Luyendyk et al.*, 1979]. Differences between the observed and predicted crustal depths can be produced thermally through a hotter mantle and/or volumetrically through increased melting and crustal thickening. In either case, these large topographic deviations from predicted subsidence curves probably resulted from changes in mantle plume activity. *Vogt* [1971, 1983] suggested that the anomalies originated under Iceland and propagated down the Reykjanes Ridge, creating a time-transgressive or V-shaped signature. Based on age versus distance relationships of the escarpments, *Vogt* [1971] estimated that the propagation rate along the ridge was ~20 cm/yr, yielding ages of ~17 and 7 Ma in Iceland for the events that formed Escarpments E (circa 14 Ma on the Reykjanes Ridge; Figure 2) and A (circa 3.5 Ma on the Reykjanes Ridge; Figure 2), respectively.

We reanalyzed the geophysical data from cruise Vema 23-03, an extensive survey of the Reykjanes Ridge [*Talwani et al.*, 1971]. The bases of Escarpments E and A were identified in eleven traverse profiles identified by *Talwani et al.* [1971] (Table 1; Figures 1 and 2). The ages for each profile were plotted versus the distance from the Icelandic Plateau, showing a clear pattern of decreasing age with distance (Figure 3). A linear regression was used to estimate the age of the event under Iceland, assuming a constant rate of propagation along the ridge axis [*Vogt*, 1971]. Our age estimate for the mantle plume event that created Escarpment E is 16.3 Ma, which is similar to Vogt's estimate (Figure 3). However, the age estimate for the base of Escarpment A from our analysis is closer to 4 Ma, not 7 Ma as Vogt suggested, indicating a much faster propagation rate of the anomaly along the ridge axis for the younger event.

Additional Ridges D, C, and B were identified by Vogt; we estimate that they originated on Iceland around 13, 9, and 7.5 Ma, respectively (Figure 3). The slope of the age versus distance from Iceland of each feature (Figure 3) is a function of the propagation rate of the plume/discharge signal down the Reykjanes Ridge. Beginning with Escarpment E, the linear regressions indicate that propagation rates increased from 16 cm/yr to 20, 33, 50, and >100 cm/yr for events that formed Ridges D, C, and B and Escarpment A, respectively (Figure 3). *White et al.* [1995] noted that mantle flow rates around Iceland varied during the past 20 m.y. However our estimates are much higher than rates typically associated with hot spot regions. If real, one possible explanation for the changing propagation rates is that the plume discharge events for the older events encountered colder crust, impeding the progression of the anomaly away from the source. The discharge from each successive event encountered hotter and less resistance crust, allowing faster propagation of the thermal or melting anomaly along the Reykjanes system.

Variations in lava growth rates on Iceland may be the subaerial response to mantle plume fluctuations. There were periods of distinctly higher growth rates in lava sequences on Iceland that are well-constrained by K-Ar dates [*Saemundsson et al.*, 1980; *McDougall et al.*, 1984; *Saemundsson*, 1986]. On the northwest peninsula, two composite sequences of lava flows form a topographic high along the northwestern edge of Iceland and represent over 4 km and 3 km of lava accumulation [*Saemundsson et al.*, 1980]. K-Ar dates indicate that average growth rates from 14 to 12 Ma were ~2 km/m.y., but growth slowed to a much lower rate of ~0.7 km/m.y. from 12 to 8 Ma (Figure 4). Two other sections recorded high lava accumulation at rates of 4 and 2.6 km/m.y. for the intervals 9.5 to 9.0 Ma and 7.5 to 6.5 Ma, respectively (Figure 4). While it is difficult to characterize the volcanic history on Iceland with individual flows, high accumulation rates in several well-dated sections indicate that intervals of high lava accumulation corresponded with intervals of high mantle plume activity extrapolated from the linear regressions in Figure 3.

The timing of the GSR response to changes in the injection of heat and buoyant mantle plume mantle into the asthenosphere below the ridge should have been similar to the timing of the events on Iceland, although there may have been minor delays between events at Iceland and the distal extent of the regional swell. Because the record of volcanic histories for Iceland and GSR is incomplete, the topography of the Reykjanes Ridge is used as a proxy for changes in the mantle plume activity. The Reykjanes Ridge chronology was adjusted to reflect the Icelandic history by using the intercepts at Iceland for each of the mantle plume events (Figure 3).

Table 1. Age Estimates for the Bathymetric Features Observed in the V23-03 Traverse Profiles

	Escarpment E		Ridge D		Ridge C		Ridge B		Escarpment A	
Traverse	West	East	West	East	West	East	West	East	West	East
Profile 1	13.58	13.09	10.75	10.40	8.13	8.41	6.23	6.11	3.56	3.55
Profile 2	13.52	13.04	10.70	10.17	7.81	7.50	5.71	5.71	3.56	3.52
Profile 3	12.82	12.73	10.43	10.02	7.50	7.52	6.07	6.01	3.40	3.16
Profile 4	12.62	12.56	10.28	10.21	7.15	7.02	5.38	5.71	3.35	3.47
Profile 5	12.48	12.55	10.35	10.02	7.14	7.16	5.78	5.38	3.36	3.28
Profile 6		12.05		9.27		7.01	5.71	5.32	3.36	3.24
Profile 7	12.19	11.76	9.22	9.01	7.14	7.41	5.01	5.62	3.55	3.31
Profile 8				9.23		6.40		6.06	3.55	3.34
Profile 9	11.74	12.00	9.68	8.92	7.27	6.88	5.18	5.16	3.31	3.44
Profile 10	11.95	11.75	9.45	8.53	6.92	6.56	5.22	5.12	3.53	3.28
Profile 11	11.57	11.38	9.41	9.32	7.26	6.71	5.98	5.77	3.36	2.92

The profile number corresponds to the designation of *Talwani et al.* [1971]. Two ages represent the east and west flanks of the Reykjanes Ridge from each profile.

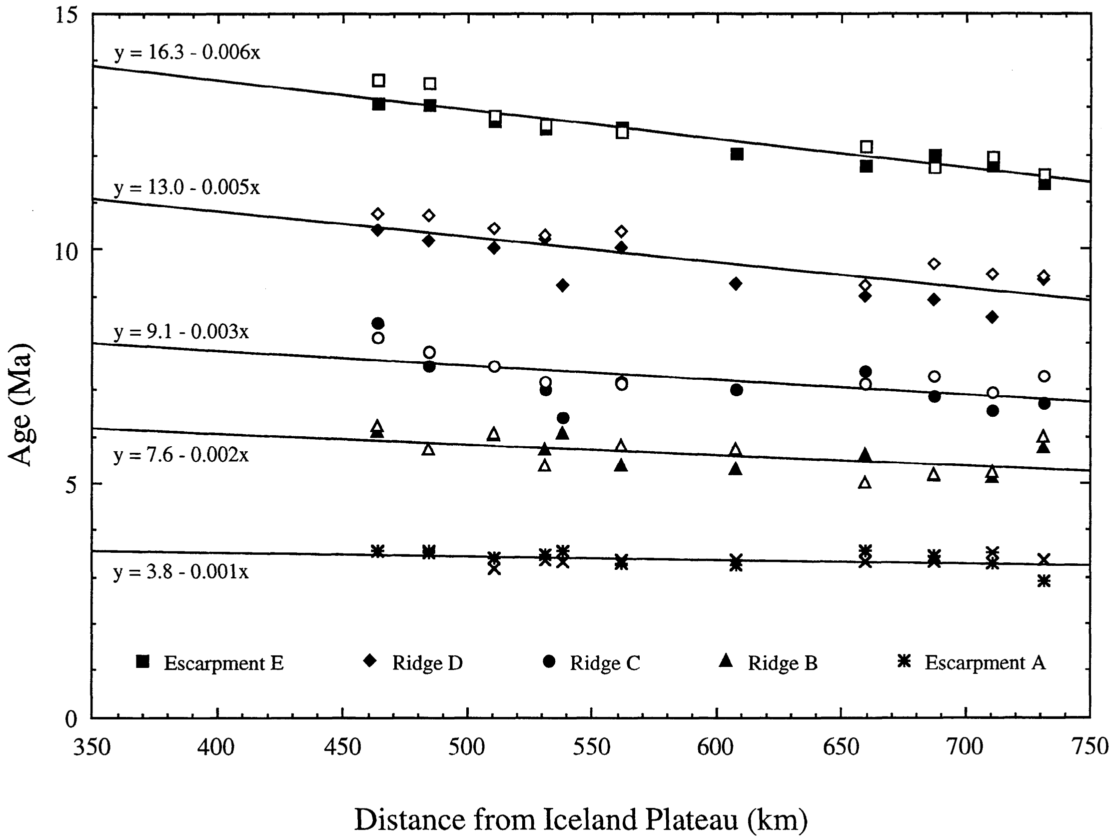

Figure 3. Age versus distance from the center of Iceland for Escarpments E and A and Ridges D, C, and B taken on cruise V23-03. Data points for each were taken from both the east and west sides of the ridge from the 11 V23-03 seismic lines across the Reykjanes Ridge. Ages for each feature were obtained by correlation of the polarity patterns to the geomagnetic polarity timescale (GPTS) (e.g., Figure 2a). The open symbols are points taken from the west side of the ridge, and the solid symbols are points taken from the east. Simple linear regressions were calculated for each bathymetric feature and are shown on the left side of Figure 3. Error analysis on the regressions estimates that the errors on the intercepts at Iceland are around 0.3 m.y. for the older events and are ~0.15 m.y for the younger events.

Neogene Deepwater Circulation Patterns in the North Atlantic

Many of the first-order deepwater circulation patterns during the Neogene have been previously documented [e.g., *Schnitker*, 1980; *Blanc and Duplessy*, 1982; *Miller and Tucholke, 1983; Miller and Fairbanks*, 1985; *Woodruff and Savin*, 1989; *Wright et al.*, 1991, 1992; *Wright and Miller*, 1993]. Most studies indicate that NCW was established during the middle Miocene and has since remained relatively strong. While there is still disagreement over the role of NCW during the early Miocene [c.f. *Woodruff and Savin*, 1989; *Wright et al.*, 1992], a growing body of evidence indicates that there was a significant phase of NCW production during the early Miocene [*Ruddiman*, 1972; *Miller and Tucholke*, 1983; *Tucholke and Mountain*, 1986; *Miller and Fairbanks*, 1985; *Wright et al.*, 1992; *Wright and Miller*, 1993]. There is also some evidence suggesting that a warm, saline water mass originated in the Tethyan Ocean during parts of the early and middle Miocene [*Woodruff and Savin*, 1989]. Below we synthesize the available evidence for deepwater circulation in the North Atlantic using benthic foraminiferal $\delta^{13}C$ records [e.g., *Bender and Keigwin*, 1979; *Miller and Fairbanks*, 1985; *Woodruff and Savin*, 1989; *Wright et al.*, 1991, 1992] and large-scale changes in sedimentation patterns in the North Atlantic [e.g., *Miller and Tucholke*, 1983; *Mountain and Tucholke*, 1985; *Tucholke and Mountain*, 1986].

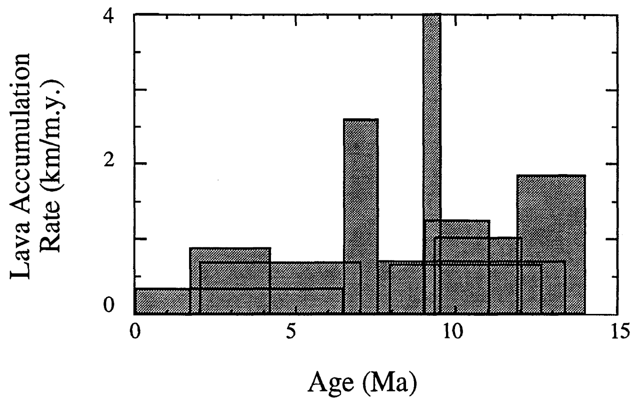

Figure 4. Rate of lava accumulation for several of the thick sections of radiometrically dated lava sequences on Iceland. The data are summarized in *Saemundson* [1986].

Neogene $\delta^{13}C$ records. Benthic foraminiferal $\delta^{13}C$ records provide one the best proxies to reconstruct Neogene deepwater circulation patterns because certain benthic foraminifera accurately record $\delta^{13}C$ variations in the dissolved inorganic carbon (DIC) reservoir [*Belanger et al.*, 1981; *Graham et al.*, 1981]. In the modern ocean, there are considerable differences in DIC $\delta^{13}C$ values, reflecting the basin-to-basin fractionation caused by deepwater circulation patterns [*Kroopnick*, 1985]. This fractionation occurs because the $\delta^{13}C$ value and nutrient content of deep/bottom waters is a function of the time the water mass has been isolated from the surface. As water masses sink and move away from their source regions, they collect organic matter which falls from the surface ocean. Oxidation of this organic matter releases CO_2 with low $\delta^{13}C$ values (-25‰) and high nutrients, lowering the DIC $\delta^{13}C$ value in the deep waters. Therefore deepwater masses proximal to source regions have high DIC $\delta^{13}C$ values and low nutrients, while more distal water masses have low DIC $\delta^{13}C$ values and high nutrients. By comparing benthic foraminiferal $\delta^{13}C$ values at various points in the deep ocean, one can determine deepwater patterns.

Neogene $\delta^{13}C$ records also reflect variations in the mean ocean DIC $\delta^{13}C$ value and the subsequent overprinting by deepwater circulation patterns (Figure 5). In fact, most of the structure observed in Neogene $\delta^{13}C$ records resulted from mean ocean DIC $\delta^{13}C$ changes. These variations reflect whole ocean $\delta^{13}C$ changes related to the input and output ratios of organic versus inorganic carbon [*Miller and Fairbanks*, 1985; *Vincent and Berger*, 1985; *Shackleton*, 1987]. Because these $\delta^{13}C$ variations were global, deepwater circulation $\delta^{13}C$ differences can be isolated by making site to site comparisons. However, several factors need to be considered before deepwater patterns can be determined. First, this procedure requires good age control for each record because mean ocean $\delta^{13}C$ changes were often rapid and larger than the circulation induced $\delta^{13}C$ differences [*Wright et al.*, 1992]. The requisite age control was achieved by using an integrated stratigraphic framework based on correlating sites with adequate polarity records to the GPTS [*Cande and Kent*, 1992], using $\delta^{18}O$ records [*Miller et al.*, 1991; *Wright and Miller*, 1992; *Wright et al.*, 1992], and published biostratigraphy [e.g., *Miller et al.*, 1985].

Magnitudes of site to site $\delta^{13}C$ differences are also partially controlled by the mean ocean nutrient level because deep-water $\delta^{13}C$ values and nutrients are coupled, independent of the prevailing deepwater circulation pattern. During intervals of lower nutrients (e.g., early and middle Miocene [*Delaney and Boyle*, 1987]), $\delta^{13}C$ differences between the deepwater end-members (i.e., North Atlantic and central Pacific) were low [*Wright et al.*, 1991]. Conversely, by the end of the Miocene, mean ocean nutrient levels and end-member $\delta^{13}C$ differences were high, similar to the modern levels. This problem was minimized by using the Southern Ocean $\delta^{13}C$ record to monitor the relative strength of the end-members. Since the opening of the Drake Passage in the Oligocene [*Lawver et al.*, 1992], the geochemical composition, including its $\delta^{13}C$ value, of the Southern Ocean reflected the mixture of the outflow from the Atlantic, Indian, and Pacific Oceans. During intervals of NCW production, the Southern Ocean $\delta^{13}C$ value was intermediate between the Atlantic and Indo-Pacific values [*Oppo and Fairbanks*, 1987; *Charles and Fairbanks*, 1992; *Wright et al.*, 1991, 1992]. During intervals of reduced NCW production, Southern Ocean $\delta^{13}C$ values became similar to the Indo-Pacific value. The Southern Ocean $\delta^{13}C$ value reflected the relative contribution from each ocean, even though nutrient/$\delta^{13}C$ variations may have changed the magnitude of the $\delta^{13}C$ difference between the Pacific and North Atlantic end-members. One important caveat is that as the end-member $\delta^{13}C$ differences decrease, the ability to estimate the relative flux from the end-members decreases as well [*Wright et al.*, 1991].

Sites used for the North Atlantic and Pacific end-members and Southern Ocean monitor are listed in Table 2. For the North Atlantic end-member, Deep Sea Drilling Project (DSDP) site 563 was largely used for the Miocene and site 552 for the Pliocene reconstructions. Gaps in the these records due to coring breaks and erosional unconformities were filled by other sites, in particular, site 608 for the Miocene and site 607 for the Pliocene intervals. The Pacific end-member was reconstructed using the records from site 289 for the Miocene and site 677 for the Pliocene. The most critical record for this approach is the Southern Ocean record. Atlantic sector sites 360 and 704 were used for the most part. However, a large middle Miocene unconformity at these sites necessitated the use of site 747 from the Indian sector of the Southern Ocean. Assumptions must be made when using one site to characterize whole ocean end-members. In the case of the North Atlantic end-member, site 563 is located well downstream (35°N) of the true North Atlantic end-member. As a result, this site is susceptible to variations in the mixing front between NCW and Southern Component Water (SCW). Conversely, site 552 is located on Rockall Plateau in the eastern North Atlantic and is upstream of the Denmark Straits overflow water, an important component of modern NADW. One complication with the southern Ocean record may have occurred during the early Miocene because of an Indian Ocean flux with a high $\delta^{13}C$ signal [*Woodruff and Savin*, 1989]. This would increase the apparent NCW flux. However, *Wright et al.* [1992] and *Wright and Miller* [1993] demonstrated that while is this possible, the first-order interpretation of NCW history from this method is consistent several other indicators for the early Miocene.

The $\delta^{13}C$ records for each end-member were stacked, interpolated to constant 0.1-m.y. intervals, and smoothed with a 11 point (±0.5 m.y.) Gaussian filter. NCW flux was estimated by using the following equation [*Oppo and Fairbanks*, 1987]:

$$\% \mathrm{NCW} = \frac{\delta^{13}C_{SO} - \delta^{13}C_{PO}}{\delta^{13}C_{N.Atl} - \delta^{13}C_{PO}} \times 100 \tag{1}$$

where SO, PO, and N.Atl refer to the Southern Ocean monitoring site and the Pacific and North Atlantic end-members. Because of minor uncertainties in age control and differences in the temporal resolution between the sites, only the first-order $\delta^{13}C$ differences (m.y.) can be interpreted with any degree of confidence. Certainly, there were higher frequency changes (orbital scale) in the climate/deepwater circulation system [e.g., *Pisias et al.*, 1985]; however, high-frequency changes were superimposed on longer-term deepwater changes.

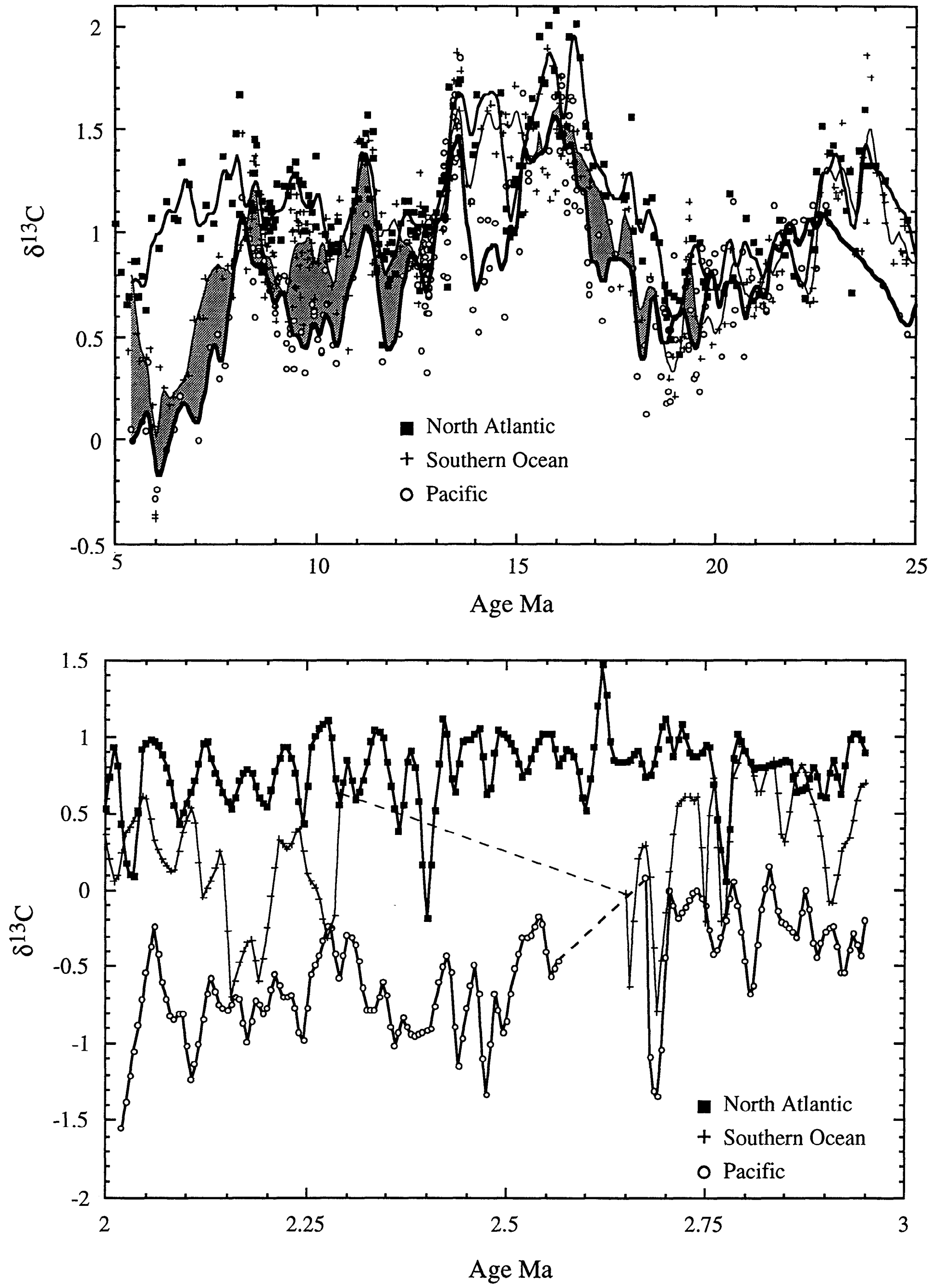

Figure 5. Composite $\delta^{13}C$ curves of the North Atlantic, Southern, and Pacific Oceans for the (a) Miocene and (b) an expanded view of the late Pliocene (see Table 2 for a summary of the data sources). For the Miocene, the North Atlantic, Pacific, and Southern Ocean $\delta^{13}C$ curves were generated by interpolating the data to constant 0.1-m.y. intervals and smoothing with a 11-point Gaussian filter. The shaded area in Figure 5a represents times when the Southern Ocean $\delta^{13}C$ value was higher relative to the Pacific $\delta^{13}C$ value, indicating Northern Component Water (NCW) production.

The first interval of NCW production during the Neogene occurred in the late early to early middle Miocene (20 to 15 Ma), reaching peak production around 17 Ma (Figure 5) [*Wright et al.*, 1992]. Northern Component Water production was reduced/eliminated around 15 Ma, before it resumed around 12.5 Ma. This phase of NCW continued through the end of the Miocene and into the Pliocene with minor interruptions/reductions around 9 and 7 Ma [*Wright et al.*, 1991, 1992]. During the Pliocene, the NCW flux was unusually high between 4 and 3 Ma, but decreased after 3 Ma (Figure 5) [*Raymo et al.*, 1990b, 1992; *Hodell and Ciesielski*, 1991]. Following this reduction, high frequency (Milankovitch) variations in NCW were particularly apparent with low NCW fluxes occurring during glacial intervals and high NCW fluxes during interglacial intervals [*Raymo et al.*, 1990b, 1992].

Table 2. Isotope Records Used to Construct the Composite $\delta^{13}C$ Curves Shown in Figure 5

Site	Time Interval	Reference
	North Atlantic	
552	0-3 Ma	*Shackleton and Hall.* [1984]; *Curry and Miller* [1989]
607	2-3 Ma	*Raymo et al.* [1992]
552	3-8 Ma	*Keigwin et al.* [1986]
563	8-25 Ma	*Miller and Fairbanks* [1985]; *Wright et al.* [1991, 1992]
	Southern Ocean	
RC13-229	0 - 0.750 Ma	*Oppo et al.* [1990]
704	0-5 Ma	*Hodell and Ciesielski* [1991]
	5-10 Ma	*Wright et al.* [1991]
	16-24 Ma	*Wright et al.* [1992]
360	5-20 Ma	*Wright et al.* [1991, 1992]
	Pacific Ocean	
677	0-5	*Shackleton and Hall* [1989] *Shackleton et al.* [1990]
289	5-25 Ma	*Savin et al.* [1981, 1985] *Woodruff et al.* [1981]

Neogene sedimentation patterns. Neogene sedimentation patterns in the North Atlantic reflect the presence of strong deep-water currents and are marked by drift development in some areas and widespread erosion in other areas [e.g., *Miller and Tucholke*, 1983; *Tucholke and Mountain*, 1986; *Thiede and Ehrmann*, 1986; *Masson and Kidd*, 1986; *Vogt and Tucholke*, 1989; *Wold*, 1994]. Accumulation on the Feni Drift began in the earliest Oligocene and has since remained relatively constant (Figure 6) [*Kidd and Hill*, 1986; *Wold*, 1994]. Since the Oligocene, there were three notable changes in the total amount of sediment accumulating in North Atlantic drifts [*Wold*, 1994]. The first of these occurred around 19 Ma with increased sedimentation on Bjorn and Gardar Drifts (Figure 6) [*Miller and Tucholke*, 1983]. Development of the Hatton and Snorri Drifts around 13 Ma produced a second increase in the accumulation of drift sediments [*Vogt and Tucholke*, 1989; *Wold*, 1994]. A large change occurred during the early Pliocene when sedimentation increased dramatically on the Eirik and Gloria Drifts [*Wold*, 1994]. The magnitude of the Pliocene increase in drift accumulation rates can in part be attributed to the increase in the sediment supply resulting from increased NHG. The development of unconformities in other areas of the North Atlantic accompanied the increases in drift accumulation [*Vogt and Tucholke*, 1989]. Three major Neogene unconformities have been extensively mapped in the North Atlantic using seismic records [*Miller and Tucholke*, 1983; *Tucholke and Mountain*, 1986; *Masson and Kidd*, 1986]. Age estimates for seismic Reflector R2 vary between 20 and 16 Ma, representing more than one erosional event during the early Miocene [e.g., *Bauldauf*, 1986; *Wright et al.*, 1992], and correspond with the development of the Bjorn and Gardar Drifts (Figure 6). Age estimates for seismic Reflectors Merlin and Blue match the middle Miocene and early Pliocene increases in drift accumulation (Figure 6). The drift accumulation and seismic data indicate that strong deepwater fluxes in the North Atlantic developed at ~ 19, ~13, and ~4 Ma [*Miller and Tucholke*, 1983; *Mountain and Tucholke*, 1985; *Vogt and Tucholke*, 1989].

Discussion

Although the role of the GSR as a possible control on deepwater history has been recognized for over 20 years [*Vogt*, 1972; *Shor and Poore*, 1979; *Luyendyk et al.*, 1979; *Miller and Wright*, 1989; *Vogt and Tucholke*, 1989; *Wright and Miller*, 1991; *Wold*, 1994], a definite link between GSR ridge and NCW formation has been wanting for two reasons. First,

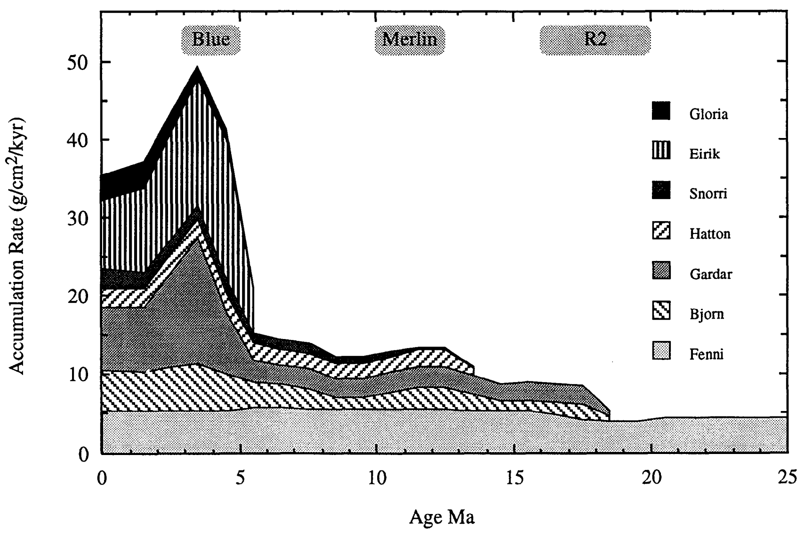

Figure 6. Summary of the accumulation of drift sediments in the North Atlantic taken from *Wold* [1994]. Reflectors R2, Merlin, and Blue are three major seismic reflectors in the North Atlantic, and their age ranges are shown at the top of the graph. Increases in the accumulation of drift sediments correspond to the age of the seismic reflectors.

there has been considerable debate over early and middle Miocene deepwater circulation patterns in the North Atlantic [c.f. *Woodruff and Savin*, 1989; *Wright et al.*, 1992], and the timing of the initiation of NCW has ranged from middle Miocene to earliest Oligocene. Our synthesis of carbon isotopic records, drift accumulation reconstructions, and distributions of unconformities indicates that there were two distinct phases of Neogene NCW production: the widely recognized middle Miocene-Pliocene interval [*Schnitker*, 1980; *Miller and Fairbanks*, 1985; *Woodruff and Savin*, 1989;*Wright et al.*, 1992] and an early Miocene pulse [*Miller and Tucholke*, 1983; *Miller and Fairbanks*, 1985; *Wright et al.*, 1992]. Second, because the mantle plume under Iceland is dynamic [*Vogt*, 1971, 1983], there was no clear mechanism linking GSR subsidence history to mantle plume fluctuations. *Vogt and Tucholke* [1989] pointed out that regional elevations may have been increased through volcanic accretion or thermal uplift. However, they lacked a mechanism linking this to the GSR because of its distance from the volcanic source and low heat flow on the GSR. Injection of buoyant mantle material beneath the crust creating a regional swell [*Sleep*, 1990] provides a mechanism linking GSR subsidence history to mantle plume activity, avoiding the problem of low heat fluxes. We establish detailed (m.y. resolution) empirical correlations between regional topographic anomalies (proxies of mantle plume activity) and deepwater history (Figure 7).

It is difficult to infer the magnitude of uplift on Iceland and along the GSR from the Reykjanes Ridge profiles; however, there is a clear link between the timing of tectonic and deep-water circulation change during the Neogene [*Vogt and Tucholke*, 1989]. Periods of high NCW production occurred during intervals of low inferred the mantle plume activity, and periods of reduced NCW production corresponded to intervals when mantle plume activity was high (Figure 7). This establishes a good correlation between GSR history and NCW production during the Neogene, although it does not establish an unequivocal causal link and there is evidence that appears to contradict the scenario. Sediments recovered from the

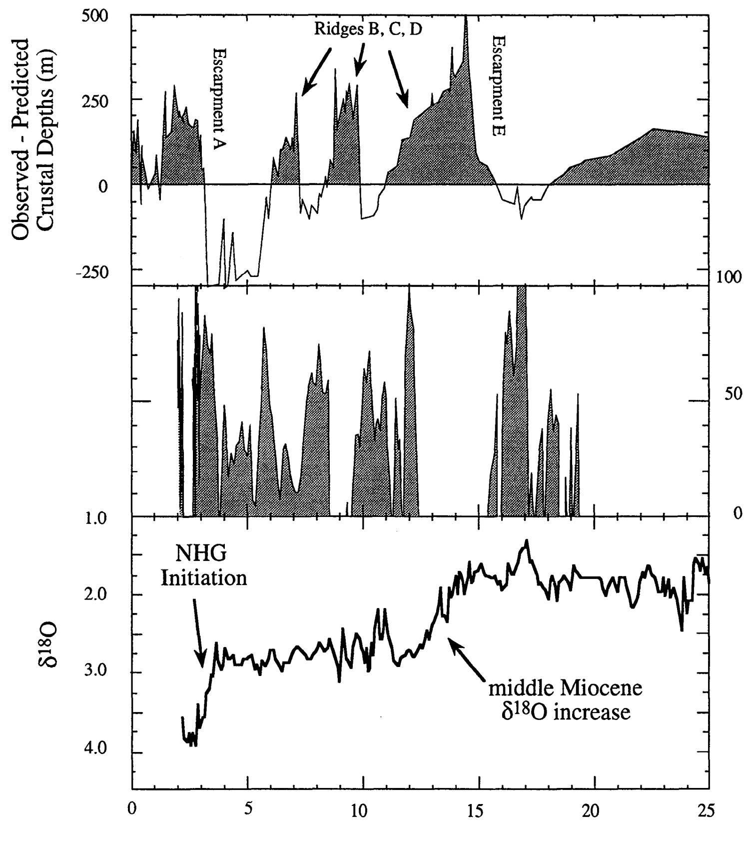

Figure 7. (a) Difference curve of the observed - predicted crustal depths for the Reykjanes and GSR cross sections shown in Figure 2b. The chronology of the Reykjanes portion of this record has been adjusted so that Escarpments E and A and Ridges D, C, and B have the ages inferred by the regressions shown in Figure 3. Positive variations through time represent increased mantle plume activity under Iceland. (b) The record of Northern Component Water flux over the past 25 m.y. estimated by recording the benthic foraminiferal $\delta^{13}C$ changes in the Southern Ocean relative to change in the North Atlantic and Pacific records. High fluxes correlate with inferred low discharge intervals. (c) Benthic foraminiferal $\delta^{18}O$ curve modified from *Wright and Miller* [1993]. The middle Miocene $\delta^{18}O$ increase and development of northern hemisphere glaciation (NHG) during the Pliocene corresponded to the development of Escarpments E and A, respectively, and changes in the flux of NCW. High-frequency variations in the NCW flux and in the $\delta^{18}O$ curves since 2.5 Ma preclude showing on these figures.

Norwegian-Greenland Seas on DSDP Leg 38 and Ocean Drilling Program (ODP) Legs 151 and 152 are equivocal about deep ventilation in this region prior to 10 Ma [*Talwani et al.*, 1976; *Larsen, et al.*, 1994; *Ocean Drilling Program Leg 151Shipboard Scientific Party*, 1994], even though virtually all studies cited here agree that NCW formation strongly influenced the North Atlantic prior to this. Labrador Sea Water (LSW) is an important component in modern NADW that forms south of the GSR; thus formation of LSW may be invoked to explain this discrepancy. However, distribution of sediment drifts and seismic disconformities points toward the Norwegian and Greenland Seas as the source of Miocene NCW [*Ruddiman*, 1972; *Roberts*, 1975; *Shor and Poore*, 1979; *Miller and Tucholke*, 1983], and the correlation between GSR history and NCW production is compelling (Figure 7) [*Vogt and Tucholke*, 1989].

Neogene Climate Connections

The establishment of a large ice sheet on Antarctica as a relatively permanent feature during the middle Miocene and development of large-scale NHG during the Pliocene were the two most significant climate changes during the Neogene [*Shackleton and Kennett*, 1975; *Savin et al.*, 1975; *Miller et al.*, 1991; *Shackleton and Opdyke*, 1977]. Equally impressive is that the climatic conditions immediately preceding these cooling events were unusually warm. Between 17 and 16 Ma, high-latitude surface and deepwater temperatures were 5° to 6°C warmer than at present, the warmest since the Eocene [*Shackleton and Kennett*, 1975; *Savin et al.*, 1975]. NCW production was high at 17 Ma but had ceased by 15 Ma (Figure 7). In the early Pliocene, several North Atlantic and Arctic localities recorded sea surface temperatures that were 4° to 8°C warmer than at present [*Dowsett and Poore*, 1991; *Cronin*, 1991]. The warm North Atlantic and Arctic Oceans during the early Pliocene coincided with a high NCW flux. The timing of these climatic events was coincident with the development of the Escarpments E and A and reduction of NCW production (Figure 7). In both the middle Miocene and Pliocene, changes in NCW production appear to have triggered major changes in global climates.

NCW production is potentially tied to climate through poleward heat transport and changes in the atmosphere's greenhouse gases [*Broecker and Denton*, 1989; *Raymo et al.*, 1990a; *Rind and Chandler*, 1991; *Imbrie et al.*, 1992; *Broecker*, 1994]. As part of NADW formation, heat is released from the ocean to the atmosphere in the high northern latitudes [*Broecker and Denton*, 1989]. Furthermore, the upwelling of NADW in the Southern Ocean is an important source of heat for the seasonal melt back of sea ice in the Southern Ocean [*Gordon*, 1981; *Jacobs et al.*, 1985]. However, General Circulation Model (GCM) results indicate that the effects of late Pleistocene variations in NCW production on global climates may have been too small («1°C) to explain the observed climatic changes [*Manabe and Stauffer*, 1988], even though certain regions experienced large changes. It is important to note, however, that these experiments considered the effects of reducing NCW from its presence flux and not the effects of a substantially higher NCW flux that occurred during the Miocene and Pliocene.

At times of unusually high NCW production (e.g., 17 to 16 Ma and 4 to 3 Ma), the poleward transport of heat through the ocean released to the atmosphere may have kept the Arctic Ocean ice-free. General Circulation Model experiments [*Raymo et al.*, 1990a; *Rind and Chandler*, 1991] suggest that no or reduced sea ice coverage in the Arctic would produce large climate effects. *Rind and Chandler* [1991] concluded that if ocean heat transports were high enough to sustain ice-free conditions in the Arctic, then the low to mid latitude surface air temperatures would change little (<1°C warmer), but the high latitudes would warm significantly (10° to 20°C during the winter). These surface air temperature differences were due primarily to sea ice differences and the associated albedo feedbacks [*Rind and Chandler*, 1991] and the ocean's increased capacity to release heat to the atmosphere [*Raymo et al.*, 1990a]. Unfortunately, it is difficult to determine the extent of sea ice in the past, and no real consensus exists regarding the presence or absence of Arctic sea ice during the Pliocene [c.f. *Clarke*, 1982; *Herman and Hopkins*, 1980].

The relationship between NCW production and climate change during the Neogene was similar to late Pleistocene patterns: high fluxes of NCW were associated with warm climates and low NCW fluxes were associated with cold climates. Although we advocate an active role for NCW in controlling climate, the long-term record of Neogene climate cannot be explained solely by deepwater changes. Neogene cooling was part of the long-term cooling in the Cenozoic that began in the early Eocene, and there is no evidence for pre-Neogene NCW other than a short pulse (<0.5 m.y.) in the earliest Oligocene [*Miller and Tucholke*, 1983; *Miller*, 1992]. The absence of NCW prior to 20 Ma was associated with warm global climates and not with glaciation as occurred in the middle Miocene. Furthermore, renewed production of NCW in the late middle Miocene (since 12 Ma) did not cause climate to return to the warm conditions that existed prior to the middle Miocene $\delta^{18}O$ increase. As for the development of NHG, the reduction of NCW at ~3 Ma cannot be solely responsible for these cycles because there is no evidence for large northern hemisphere ice sheets during the middle Miocene shutdown of NCW. Therefore NCW production cannot be the sole control on Neogene climates; it must be a secondary effect that overprinted a long-term global cooling trend.

There are three basic categories of models that attempt to explain the long-term Cenozoic cooling: (1) decreased poleward heat flow through the ocean; (2) disruption of atmospheric circulation patterns; and (3) decreases in greenhouse gas levels (CO_2, methane, and/or water vapor). A poleward flow of warm saline deep water (WSDW) that originated in the low latitudes and upwelled in the high southern latitudes has been proposed to explain the unusually warm climates of the early Cenozoic [*Woodruff and Savin*, 1989; *Kennett and Stott*, 1990]. While there is some evidence for periodic existence of WSDW during the Cenozoic, existing records of WSDW production show little to no correlation of WSDW with Cenozoic climate change [*Wright and Miller*, 1993], and we conclude that decreased ocean heat transport cannot explain the global cooling since the early Eocene (see also *Sloan et al.* [1995]).

Recent studies have emphasized the role of uplift in global cooling [e.g., *Raymo and Ruddiman*, 1992]. The Tibetan and

Colorado Plateaus as well as several mountain ranges recorded dramatic increases in uplift rates during the Neogene. One important consequence of plateau uplift is a disruption of atmospheric circulation patterns [*Manabe and Terpstra*, 1974; *Ruddiman et al.*, 1989] which could lead to the initiation of glacial/interglacial cycles and changes in the evaporation-precipitation balance in potential deepwater source regions [*Ruddiman et al.*, 1989]. Another possible consequence of plateau uplift is increased continental weathering and draw down of atmospheric CO_2 concentrations [e.g., *Raymo et al.*, 1988; *Raymo*, 1994]. The increase in oceanic $^{87}Sr/^{86}Sr$ values may have been caused by increased continental weathering, most of which can be attributed to uplift in the Himalayan/Tibetan region. While mountain uplift is still a viable hypothesis, we suggest that change in water vapor transport may be the key to the long-term Cenozoic cooling.

Although there is no definite proxy for the most important greenhouse gas, water vapor, we suggest that a decrease in Cenozoic water vapor may have been an important contributor to the general cooling. The main source regions for water vapor, the subtropical and tropical oceans, have decreased in area throughout the Cenozoic [*Barron*, 1985]. The most dramatic increase in land area during the Cenozoic occurred with the systematic closure of the highly evaporative Tethyan Ocean from the Eocene to the middle Miocene. The feedbacks associated with a decrease in atmospheric water vapor may be as important as decreasing the sources. As the atmosphere cools, its ability to hold water vapor is decreased, causing further cooling to some degree. While this approximation of Cenozoic atmospheric water vapor is crude, it is consistent with the idea that decreased water vapor preconditioned the high latitudes to be more sensitive to changes in NCW production.

It is clear that the long-term climate cooling during the Cenozoic must be attributed to factors other than NCW production. It can be argued that climate controlled NCW fluxes during the Neogene with high NCW fluxes during warm intervals, similar to the Plio-Pleistocene patterns [*Raymo et al.*, 1992; *Wright et al.*, 1991]. Either one or all processes discussed above may have preconditioned the mid to high-latitude regions to have been more susceptible to a decrease in meridional heat transport associated with changes in NCW production. However, high NCW fluxes have positive feedbacks on climate, particularly in the high northern latitudes. Even though the long-term control of climate is governed by other factors, the unusually warm climate centered at 17 and 3 Ma appears to be related to the high NCW fluxes at those times (Figure 7). Reduced NCW fluxes that followed each of these maxima allowed the normal progression of climate cooling: the development of a permanent ice sheet on Antarctica during the middle Miocene and large-scale NHG during the late Pliocene. If this is the case, then the link between NCW and mantle plume activity also establishes a connection between climate and marine tectonics.

Conclusions

The bathymetric features along the Reykjanes Ridge originally identified by *Vogt* [1971] resulted from increases in the flux of buoyant material within the Icelandic Hot Spot during the Neogene. The V-shaped pattern associated with these escarpments and ridges represents the time-transgressive propagation along the ridge axis. The age versus distance relationship for each of these topographic features or crustal anomalies was used to determine the time of origin on Iceland and rate of propagation. The largest events that produced Escarpment E and A occurred on Iceland around 16 and 4 Ma, respectively. The smaller events, Ridges D, C, and B, have age estimates of 13, 9, and 7 Ma, respectively. The propagation rate of the mantle plume anomaly along the Reykjanes Ridge axis increased with each successive event from ~16 cm/yr (Escarpment E) to >100 cm/yr (Escarpment A). This may indicate that the resistance within the ridge axis was reduced during each successive event.

The GSR was also affected by the Icelandic mantle plume activity because the radial extent of the topographic swell associated with this hot spot is on the order 1000 km. Overflow waters that form NCW are sensitive to even small changes in the ridge depths. Reconstructions of Neogene deepwater circulation patterns show that reductions in NCW production occurred when mantle plume activity under Iceland was high. The flux of NCW resumed once the anomalous pulse of buoyant mantle material ceased.

The role of NCW production in long-term climate change during the Neogene is not clear. However, it appears that NCW production is at least an important feedback that augments climate change. The climatic optima during the early middle Miocene and Pliocene occurred while the production of NCW was high. The reduction of NCW as the result of uplift along the GSR may have triggered the development of a permanent Antarctic ice sheet and large-scale NHG.

Acknowledgments. We thank, P. Vogt, M. Katz, J. Zachos, and an anonymous reviewer for critical reviews which improved this manuscript greatly. Discussions with R. Buck concerning the mantle dynamics in the Iceland region and D. Kent on Iceland lava flows were very helpful. This manuscript was supported by OCE88-19438 to KGM and OCE91-17667 to JDW. This is LDEO contribution number 5452.

References

Anderson, R.N., D.P. McKenzie, and J.G. Sclater, Gravity, bathymetry, and convection in the Earth, *Earth Planet. Sci. Lett.*, *18*, 391-407, 1973.

Barron, E.J., Explanation of the Tertiary global cooling trend, *Palaeogeogr., Palaeoclimatol., Palaeoecol.*, *50*, 45-61, 1985.

Bauldauf, J. G., Biostratigraphic and paleoceanographic interpretation of lower and middle Miocene sediments, Rockall Plateau region, North Atlantic Ocean, *Initial Rep. Deep Sea Drill. Proj.*, *94*, 1033-1043, 1986.

Belanger, P. E., W. B. Curry, and R. K. Matthews, Core-top evaluation of benthic foraminiferal isotopic ratios for paleo-oceanographic interpretations, *Paleogeogr. Palaeoclimatol. Palaeoecol.*, *33*, 205-220, 1981.

Bender, M.L., and L.D. Keigwin, Speculations about the upper Miocene change in abyssal Pacific dissolved bicarbonate $\delta^{13}C$, *Earth Planet. Sci. Lett.*, *45*, 383-393, 1979.

Berger, W.H., E. Vincent, and H. Thierstein, The deep-sea record: Major steps in Cenozoic ocean evolution, in *The Deep Sea Drilling Project: A Decade of Progress*, edited by J. Warme et al., pp. 489-504, Soc. for Econ. Paleontol. and Mineral., Tulsa, Okla., 1981.

Berner, R.A., A.C. Lasaga, and R.M. Garrels, The carbonate-silicate geochemical cycle and its effect on atmospheric carbon dioxide over the past 100 million years, *Am. J. Sci*, *283*, 641-683, 1983.

Blanc, P.-L., and J. C. Duplessy, The deep-water circulation during the Neogene and the impact of the Messinian salinity crisis, *Deep Sea Res., 29 Part A,* 1391-1414, 1982.

Bohrmann, G., R. Henrich, and J. Thiede, Miocene to Quaternary paleoceanography in the northern North Atlantic: Variability in carbonate and biogenic opal accumulation, in *Geological History of the Polar Oceans: Arcitc Versus Antarctic*, edited by U. Bleil and J. Thiede, pp. 647-675, Kluwer Acad., Norwell, Mass., 1991.

Broecker, W.S., Massive iceberg discharges as triggers for global climate change, *Nature, 372,* 421-424, 1994.

Broecker, W.S., and G.H. Denton, The role of ocean-atmosphere reorganizations in glacial cycles, *Geochim. Cosmochim. Acta, 53,* 2465-2501, 1989.

Cande, S.C., and D.V. Kent, A new geomagnetic polarity time scale for the Late Cretaceous and Cenozoic, *J. Geophys. Res., 97,* 13,917-13,951, 1992.

Charles, C. D., and R. G. Fairbanks, Evidence from Southern Ocean sediments for the effect of North Atlantic deep-water flux on climate, *Nature, 355,* 416-419, 1992.

Clarke, D.L., Origin, nature and world climate effect of Arctic Ocean ice cover, *Nature, 300,* 321-325, 1982.

Cronin, T.M., Pliocene shallow water paleoceanography of the North Atlantic Ocean based on marine ostracodes, *Quat. Sci. Rev., 10,* 175-188, 1991.

Curry, W.B. and K.G. Miller, Oxygen and carbon isotopic variation in Pliocene benthic foraminifers of the equatorial Atlantic, *Proc. Ocean Drill. Program ODP Sci. Results, 108B,* 157-166, 1989.

Delaney M. L., and E. A. Boyle, Cd/Ca in late Miocene benthic foraminifera and changes in the global organic carbon budget, *Nature, 330,* 156-159, 1987.

Dowsett, H.J., and R.Z. Poore, Pliocene sea surface temperatures of the North Atlantic Ocean at 3.0 Ma, *Quat. Sci. Rev., 10,* 189-204, 1991.

Graham, D. W., B. H. Corliss, M. L. Bender, and L. D. Keigwin, Carbon and oxygen isotopic disequilibria of Recent benthic foraminifera, *Mar. Micropaleontol., 6,* 483-497, 1981.

Gordon, A.L., Seasonality of Southern Ocean sea ice, *J. Geophys. Res., 86,* 4193-4197, 1981.

Herman, Y., and D.M. Hopkins, Arctic oceanic climate in late Cenozoic time, *Science, 209,* 557-562, 1980.

Hodell, D.A., and P.F. Ciesielski, Southern Ocean response to the intensification of Northern Hemisphere Glaciation at 2.4 Ma, in *Geological History of the Polar Oceans: Arctic Versus Antarctic*, edited by U. Bleil and J. Thiede, pp. 707-728, Kluwer Acad., Norwell, Mass., 1991.

Imbrie, J., et al., On the structure and origin of major glaciation cycles, 1, Linear responses to Milankovitch forcing, *Paleoceanography, 7,* 701-738, 1992.

Jacobs, S.S., R.G. Fairbanks, and Y. Horibe, Origin and evolution of water masses near the Antarctic continental margin: Evidence from $H_2{}^{18}O/H_2{}^{16}O$ ratios in seawater , in *Oceanology of the Antarctic Continental Shelf, Antartc. Res. Ser.,* vol. 43, edited by S.S. Jacobs, pp. 59-85, AGU, Washington, D.C., 1985.

Jones, E.J., M. Ewing, J.I. Ewing, and S.L. Ettreim, Influences of Norwegian Sea overflow water on sedimentation in the northern North Atlantic and Labrador Sea, *J. Geophys, Res., 75,* 1655-1680, 1970.

Keigwin, L.D., M.-P. Aubry, and D.V. Kent, North Atlantic late Miocene stable-isotope stratigraphy, biostratigraphy, and magnetostratigraphy, *Initial Rep. Deep Sea Drill. Proj., 94,* 935-963, 1986.

Kennett, J.P. and L.D. Stott, Proteus and Proto-Oceanus: Paleogene Oceans as revealed from Antarctic stable isotopic results; ODP Leg, 113, *Proc. Ocean Drill. Program Sci. Results, 113,* 865-880, 1990.

Kidd, R.B., and P.R. Hill, Sedimentation on Feni and Gardar sediment drifts, *Initial Rep. Deep Sea Drill. Proj., 94,* 1217-1244, 1986.

Kroopnick, P., The distribution of ^{13}C of ΣCO_2 in the world oceans, *Deep Sea Res., 32,* 57-84, 1985.

Larsen, B., Geology of the Greenland-Iceland Ridge in the Denmark Strait, in *Structure and Development of the Greenland-Scotland Ridge,* edited by M. H. P. Bott et al., pp. 425-444, Plenum, New York, 1983.

Larsen, H.C., A.D. Saunders, P.D. Clift, et al., *Proceedings of the Ocean Drilling program, Initial Reports, vol. 152,* 977pp., Ocean Drill. Program, College Station Tex., 1994.

Lawver, L. A., L. M. Gahagan, and M. F. Coffin, The development of paleoseaways around Antarctica, in *The Antarctic Paleoenvironment: A Perspective on Global Change, Part 1, Antarct. Res. Ser.,* vol. 56, edited by J.P. Kennett and D. Warnke, pp. 7-30, AGU, Washington D.C., 1992.

Luyendyk, B.P., A. Shor, and J.R. Cann, General implications of the Leg 49 drilling program for North Atlantic ocean geology, *Initial Rep. Deep Sea Drill. Proj., 49,* 825-840, 1979.

Manabe, S., and R.J. Stauffer, Two stable equilibria of a coupled ocean-atmosphere model, *J. Climate, 1,* 841-866, 1988.

Manabe, S., and T.B. Terpstra, The effects of mountains on the general circulation of the atmosphere as identified by numerical experiments, *J. Atmos. Sci., 31,* 3-42, 1974.

Masson, D.G., and R.B. Kidd, Revised Tertiary seismic stratigraphy of the southern Rockall Trough, *Initial Rep. Deep Sea Drill. Proj., 94,* 1117-1126, 1986.

McDougall, I., L.Kristjansson, and K. Saemundsson, Magnetostratigraphy and geochronology of northwest Iceland, *J. Geophys. Res., 89,* 7029-7060, 1984.

Miller, K.G., Middle Eocene to Oligocene stable isotopes, climate, and deep-water history: The terminal Eocene Event?, in *Eocene-Oligocene Climatic and Biotic Evolution*, edited by D. Prothero and W.A. Berggren, pp., 160-177, Princeton University, Princeton, New Jersey, 1992.

Miller, K.G., and R.G. Fairbanks, Oligocene to Miocene carbon isotope cycles and abyssal circulation changes, in *The Carbon Cycle and Atmospheric CO_2: Natural Variations Archean to Present., Geophys. Monogr. Ser.,* vol. 32, edited by E. T. Sunquist and W. S. Broecker, pp. 469-486, AGU, Washington, D. C., 1985.

Miller, K.G., and B.E. Tucholke, Development of Cenozoic abyssal circulation south of the Greenland-Scotland Ridge, in *Structure and Development of the Greenland-Scotland Ridge,* edited by M. H. P. Bott et al., pp. 549-589, Plenum, New York, 1983.

Miller, K.G., and J.D. Wright, Subsidence history of the Greenland-Scotland Ridge revisited: Implications of uplift on deep-water circulation history, paper presented at the International Geologic Congress, Washington D.C., 1989.

Miller, K. G., M-.P. Aubrey, M. J. Khan, A. J. Melillo, D. V. Kent, and W. A. Berggren, Oligocene-Miocene biostratigraphy, magnetostratigraphy and isotopic stratigraphy of the western North Atlantic, *Geology, 13,* 257-261, 1985.

Miller, K.G., J.D. Wright, and R.G. Fairbanks, Unlocking the icehouse: Oligocene-Miocene oxygen isotope, eustasy, and margin erosion, *J. Geophys. Res., 96,* 6829-6848, 1991.

Molnar, P., and P. England, Late Cenozoic uplift of mountain ranges and global climate change: Chicken or egg?, *Nature, 346,* 29-34, 1990.

Mountain, G.S., and B.E. Tucholke, Mesozoic and Cenozoic Geology of the U.S. Atlantic continental slope and rise, in *Geologic Evolution of the United States Atlantic Margin,* edited by C.W. Poag, pp. 293-341, Van Nostrand Reinhold Company, New York, 1985.

Nunns, A.G., Plate tectonic evolution of the Greenland-Scotland Ridge and surrounding regions, in *Structure and Development of the Greenland-Scotland Ridge,* edited by M. H. P. Bott et al., pp. 11-30, Plenum, New York, 1983.

Ocean Drilling Program Leg 151 Shipboard Scientific Party, Exploring Arctic history through scientific drilling, *Eos Trans. AGU, 75,* 281, 1994.

Oppo, D.W., and R.G. Fairbanks, Variability in the deep and intermediate water circulation of the Atlantic Ocean during the past 25,000 years: Northern Hemisphere modulation of the Southern Ocean, *Earth Planet. Sci. Lett., 86,* 1-15, 1987.

Oppo, D.W., R.G. Fairbanks, and A.L. Gordon, Late Pleistocene Southern Ocean $\delta^{13}C$ variability, *Paleoceanography, 5,* 43-54, 1990.

Pisias, N. G., N. J. Shackleton, and M.A . Hall, Stable isotope anc calcium carbonate records from hydraulic piston cored Hole 574A: high-resolution records from the middle Miocene, *Initial Rep. Deep Sea Drill. Proj., 85,* 735-748, 1985.

Raymo, M.E., The Himalayas, organic carbon burial, and climate in the Miocene, *Paleoceanography, 9,* 399-404, 1994.

Raymo, M.E., and W.F. Ruddiman, Tectonic forcing of late Cenozoic climate, *Nature, 359*, 117-122, 1992.

Raymo, M.E., W.F. Ruddiman, and P.N. Froelich, Influence of late Cenozoic mountain building on ocean geochemical cycles, *Geology, 16*, 649-653, 1988.

Raymo, M. E., W. F. Ruddiman, J. Backman, B. M. Clement, and D. G. Martinson, Late Pliocene variation in northern hemisphere ice sheets and North Atlantic Deep Water circulation, *Paleoceanography, 4*, 413-446, 1989.

Raymo, M.E., D. Rind, and W.F. Ruddiman, Climatic effects of reduced arctic sea ice limits in the GISS II General Circulation Model, *Paleoceanography 5*, 367-382, 1990a.

Raymo, M.E., W.F. Ruddiman, N.J. Shackleton, and D.W. Oppo, Evolution of Atlantic-Pacific $\delta^{13}C$ gradients over the last 2.5 m.y., *Earth Planet. Sci. Lett., 97*, 353-368, 1990b.

Raymo, M.E., D. Hodell, and E. Jansen, Response of deep ocean circulation to initiation of Northern Hemisphere Glaciation (3-2 Ma), *Paleoceanography, 7*, 645-672 1992.

Ridd, M.F., Aspects of the Tertiary geology of the Faeroe-Shetland Channel, in *Structure and Development of the Greenland-Scotland Ridge,* edited by M. H. P. Bott et al., pp. 91-108, Plenum, New York, 1983.

Rind, D., and M. Chandler, Increased ocean heat transports and warmer climate, *J. Geophys Res., 96*, 7437-7461, 1991.

Roberts, D.G., Tectonic and stratigraphic evolution of the Rockall Plateau and Trough, in *Petroleum and the Continental Shelf of Northwest Europe*, vol. 1, *Geology*, edited by A.W. Woodland, pp. 77-89, Appl. Sci., Essex, England, 1975.

Ruddiman, W.F., Sediment redistribution on the Reykjanes Ridge: Seismic evidence, *Geol. Soc. Am. Bull., 83*, 2039-2062, 1972.

Ruddiman, W.F., W.L. Prell, and M.E. Raymo, Late Cenozoic uplift in southern Asia and the American West: Rationale for General Circulation Modeling Experiments, *J. Geophys, Res.*, 94, 18,379-18,391 (1989).

Saemundsson, K., Subaerial volcanism in the western North Atlantic, in *Decade of North American Geology, vol. M, The Western North Atlantic Region*, edited by P.R. Vogt and B.E. Tucholke, pp. 69-86, Geol. Soc. of Am., Boulder, Colo., 1986.

Saemundsson, K., L. Kristjansson, I. McDougall, and N.D. Watkins, K-Ar dating, geological and paleomagnetic study of a 5-km lava succession in northern Iceland, *J. Geophys. Res., 85*, 3628-3646, 1980.

Savin, S.M., R.G. Douglas, and F.G. Stehli, Tertiary marine paleotemperatures, *Geol. Soc. Am. Bull., 86*, 1499-1510, 1975.

Savin, S.M., G. Keller, R.G. Douglas, J.S. Killingley, L. Shaughnessy, M.A. Sommer, E. Vincent, and F. Woodruff, Miocene benthic foraminiferal isotope records: A synthesis, *Mar. Micropaleontol., 6*, 423-450, 1981.

Savin, S.M., et al., The evolution of Miocene surface and near-surface marine temperatures: Oxygen isotopic evidence, in *The Miocene Ocean: Paleoceanography and Biogeography*, edited by J.P. Kennett (ed.),*Mem. Geol. Soc. Am., 163*, 49-82, 1985.

Schilling, J.-G., Geochemical and isotopic variation along the Mid-Atlantic Ridge axis from 79°N to 0°N, in *Decade of North American Geology, vol. M, The Western North Atlantic Region*, edited by P.R. Vogt and B.E. Tucholke, pp. 137-156, Geol. Soc. Am., Boulder, Colo., 1986.

Schnitker, D., North Atlantic oceanography as possible cause of Antarctic glaciation and eutrophication, *Nature, 284*, 615-616, 1980.

Sclater, J.G., R.N. Anderson, and N.L. Bell, Elevation of ridges and evolution of the central eastern Pacific, *J. Geophys. Res., 76*, 7888-7915, 1971.

Shackleton, N.J., The carbon isotope record of the Cenozoic: History of organic carbon burial and of oxygen in the ocean and atmosphere, in *Marine Petroleum Source Rocks*, edited by H. Brooks and A. J. Fleet, pp. 423-434, Blackwell Sci., Cambridge, Mass., 1987.

Shackleton, N.J., and M.A. Hall, Oxygen and carbon isotope stratigraphy of Deep Sea Drilling Project Hole 552A: Plio-Pleistocene glacial history, *Initial Rep. Deep Sea Drill. Proj., 81*, 599-610, 1984.

Shackleton, N.J., and M.A. Hall, Stable isotope history of the Pleistocene at ODP Site 677, *Proc. Ocean Drill. Program Sci. Results, 111*, 295-316, 1989.

Shackleton, N.J., and J. P. Kennett, Paleotemperature history of the Cenozoic and initiation of Antarctic glaciation: Oxygen and carbon isotopic analyses in DSDP Sites 277, 279, and 281, *Initial Rep. Deep Sea Drill. Proj., 29*, 743-755, 1975.

Shackleton, N.J., and N.D. Opdyke, Oxygen isotope and paleomagnetic evidence for early Northern Hemisphere Glaciation, *Nature, 270*, 216-219, 1977.

Shackleton, N.J., et al., Oxygen isotope calibration of the onset of ice-rafting and history of glaciation in the North Atlantic region, *Nature, 307*, 620-623, 1984.

Shackleton, N.J., A. Berger, and W.R. Peltier, An alternative astononmical calibration of the lower Pleistocene timescale based on ODP Site 677, *Trans. R.Society Edinburgh Earth Sciences, 81*, 251-261, 1990.

Shor, A. N., and R. Z. Poore, Bottom currents and ice rafting in the North Atlantic: Interpretation of Neogene depositional environment of Leg 49 cores, *Initial Rep. Deep Sea Drill. Proj., 49*, 859-872, 1979.

Sleep, N.H., Hotspots and mantle plumes: Some phenomenology, *J. Geophys. Res., 95*, 6715-6739, 1990.

Sloan, L.C., J.C.G. Walker, and T.C. Moore Jr., Possible role of oceanic heat transport in early Eocene climate, *Paleoceanography, 10*, 347-356, 1995.

Talwani, M., and O. Eldholm, Evolution of the Norwegian-Greenland Sea, *Geol. Soc. Am. Bull., 88*, 969-999, 1977.

Talwani, M., C.C. Windisch, and M.G. Langseth Jr., Reykjanes Ridge Crest: A detailed geophysical study, *J. Geophys. Res., 76*, 473-517, 1971.

Talwani, M., et al., *Initial Reports Deep Sea Drilling Project*, vol 38, U.S. Govt. Print. Off., Washington, D.C., 1976.

Thiede, J., and W.U. Ehrmann, Late Mesozoic and Cenozoic sediment flux to the central North Atlantic Ocean, in *North Atlantic Palaeoceanography*, edited by C.P. Summerhayes and N.J. Shackleton, pp. 3-15, Blackwell Sci., Cambridge, Mass., 1986.

Thiede, J., and O. Eldholm, Speculations about the paleodepth of the Greenland-Scotland Ridge during late Mesozoic and Cenozoic times, in *Structure and Development of the Greenland-Scotland Ridge,* edited by M.H.P. Bott, S. Saxov, M. Talwani, and J. Thiede, pp. 445-456, Plenum Press, New York, 1983.

Tucholke, B.E. and G.S. Mountain, Tertiary paleoceanography of the western North Atlantic ocean, in *Decade of North American Geology, vol. M, The Western North Atlantic Region*, edited by P.R. Vogt and B.E. Tucholke, pp. 631-650, Geol. Soc. of Am., Boulder, Colo., 1986.

Vincent, E., and W.H. Berger, Carbon dioxide and polar cooling in the Miocene: The Monterey Hypothesis, in *The Carbon Cycle and Atmospheric CO_2: Natural Variations Archean to Present, Geophys. Monogr. Ser.*, vol. 32, edited by E.T. Sunquist and W.S. Broecker, pp. 455-468, AGU, Washington, D. C., 1985.

Vogt, P.R., Asthenosphere motion recorded by the ocean floor south of Iceland, *Earth Planet. Sci. Lett., 13*, 153-160, 1971.

Vogt, P.R., The Faeroe-Iceland-Greenland Aseismic Ridge and the Western Boundary Undercurrent, *Nature, 239*, 79-81, 1972.

Vogt, P.R., The Iceland phenomenon: Imprints of a hot spot on the ocen crust, and implications for flow below the plates, in *Geodynamics of Iceland and the North Atlantic Areas*, edited by L. Kristjansson, pp. 105-126, D. Reidel, Norwell, Mass., 1974.

Vogt, P.R., The Iceland mantle plume: Status of the hypothesis after a decade of new work, in *Structure and Development of the Greenland-Scotland Ridge,* edited by M.H.P. Bott, S. Saxov, M. Talwani, and J. Thiede, pp. 191-213, Plenum Press, New York, 1983.

Vogt, P.R., and O.E. Avery, Detailed magnetic surveys in the northeast Atlantic and Labrador Sea, *J. Geophys. Res., 79*, 363-389, 1974.

Vogt, P.R., and B.E. Tucholke, North Atlantic Ocean basin: Aspects of geologic structure and evolution, in *The Geology of North America,* Vol. A, *An Overview*, edited by A.W. Bally and A.R. Palmer, pp. 53-80, Geol. Soc. of Am., Boulder, Colo., 1989.

Vogt, P.R., R.K. Perry, R.H. Feden, H.S. Fleming, and N.Z. Cherkis, The Greenland-Norwegian Sea and Iceland environment: Geology and geophysics, in *The Ocean Basins and Margins*, vol. 5, edited by A.E.M. Nairn et al., pp. 493-598, Plenum, New York, 1981.

White, R., and D. McKenzie, Magmatism at rift zones: The generation of volcanic continental margins and flood basalts, *J. Geophys. Res. 94*, 7685-7729, 1989.

White, R.,S., J.W. Bowin, and J.R. Smallwood, The temperature of the Iceland plume and origin of outward-propagating V-shaped ridges, *J. Geol. Soc., 152*, 1039-1045, 1995.

Wold, C.N., Cenozoic sediment accumulation on drifts in the northern North Atlantic, *Paleoceanography, 9*, 917-941, 1994.

Woodruff, F., and S.M. Savin, Miocene deepwater oceanography, *Paleoceanography, 4*, 87-140, 1989.

Woodruff, F., S.M. Savin, and R.G. Douglas, A Miocene stable isotopic record: A detailed deep Pacific ocean study and its paleoclimatic implications, *Science, 212*, 665-668, 1981.

Wright, J. D., and K. G. Miller, Miocene stable isotope stable isotope stratigraphy, Site 747, Kerguelen Plateau, *Proc. Ocean Drill. Program, Sci. Results, 120*, 855-866, 1992.

Wright, J.D., and K.G. Miller, Greenland-Scotland Ridge subsidence and Cenozoic climate change: A tectonic alternative to Himalayan uplift, *Eos Trans. AGU, 72* (44), Fall Mett. Suppl., 258, 1991.

Wright, J.D, and K.G. Miller, Southern Ocean influences on late Eocene to Miocene deep-water circulation, in *The Antarctic Paleoenvironment: A Perspective on Global Change, Part 2, Antarct. Res. Ser.*, vol. 60, edited by J.P. Kennett and D. Warnke, pp. 1-25, AGU, Washington D.C., 1993.

Wright, J.D, K.G. Miller, and R.G. Fairbanks, Evolution of deep-water circulation: Evidence from the late Miocene Southern Ocean, *Paleoceanography, 6*, 275-290, 1991.

Wright, J.D, K.G. Miller, and R.G. Fairbanks, Miocene stable isotopes: Implications for deepwater circulation and climate, *Paleoceanography, 7*, 357-389, 1992.

K. G. Miller, Department of Geological Sciences, Rutgers University, Piscataway, NJ 08855. (e-mail: kgm@rci.rutgers.edu)

J. D. Wright, Sawyer Envirnomental Research Center, Room 236, University of Maine, Orono, ME 04469. (e-mail: jwright@maine.maine.edu)

(Received February 6, 1995; revised November 17, 1995; accepted November 30, 1995.)